

## A gauge invariant dressed holon and spinon description of the normal state of underdoped cuprates

This article has been downloaded from IOPscience. Please scroll down to see the full text article.

2004 J. Phys.: Condens. Matter 16 343

(<http://iopscience.iop.org/0953-8984/16/3/014>)

View [the table of contents for this issue](#), or go to the [journal homepage](#) for more

Download details:

IP Address: 129.252.86.83

The article was downloaded on 28/05/2010 at 07:50

Please note that [terms and conditions apply](#).

# A gauge invariant dressed holon and spinon description of the normal state of underdoped cuprates

Shiping Feng, Jihong Qin and Tianxing Ma

Department of Physics, Beijing Normal University, Beijing 100875, People's Republic of China

Received 5 August 2003, in final form 12 November 2003

Published 9 January 2004

Online at [stacks.iop.org/JPhysCM/16/343](http://stacks.iop.org/JPhysCM/16/343) (DOI: 10.1088/0953-8984/16/3/014)

## Abstract

A partial charge–spin separation fermion–spin theory is developed to study the normal-state properties of the underdoped cuprates. In this approach, the physical electron is decoupled as a gauge invariant dressed holon and spinon, with the dressed holon behaving like a spinful fermion, representing the charge degree of freedom together with the phase part of the spin degree of freedom, while the dressed spinon is a hard-core boson, representing the amplitude part of the spin degree of freedom. The local electron constraint for single occupancy is satisfied. Within this approach, the charge and spin dynamics of the underdoped cuprates are studied based on the  $t-t'-J$  model. It is shown that the charge dynamics is mainly governed by the scattering from the dressed holons due to the dressed spinon fluctuation, while the scattering from the dressed spinons due to the dressed holon fluctuation dominates the spin dynamics.

## 1. Introduction

After over fifteen years of intense experimental studies of doped cuprate superconductors, a significant body of reliable and reproducible data has been accumulated by using many probes [1, 2], which shows that the most remarkable expression of the nonconventional physics is found in the normal state [1, 2]. The normal-state properties exhibit a number of anomalous properties in the sense that they do not fit in the conventional Fermi-liquid (FL) theory [2–4], and are closely related to the fact that these materials are doped Mott insulators [1–4]. The ground state in the undoped case is an antiferromagnetic (AF) long-range-order (AFLRO) Néel state, but changing the carrier concentration by ionic substitution or increasing the oxygen content turns these compounds into strongly correlated metals leaving the AF short-range-order correlation still intact [1, 2]. It is then not surprising that the nonconventional behaviours are most striking in the underdoped regime, where the concentration of doped holes is small. The anomalous properties observed in a variety of experiments, such as the nuclear magnetic resonance (NMR), nuclear quadrupole resonance (NQR), muon spin rotation ( $\mu$ SR) techniques, inelastic neutron scattering studies [5–10], optical and transport measurements [11–14], and angle-resolved photoemission spectroscopy

(ARPES) investigation [15], exclude conventional theories. The single common feature in doped cuprates is the two-dimensional (2D)  $\text{CuO}_2$  plane [1, 2], and it seems evident that the nonconventional behaviours are dominated by this plane. Very soon after the discovery of high-temperature superconductivity (HTSC) in doped cuprates, Anderson proposed a scenario of HTSC based on the charge–spin separation (CSS) in 2D [3], where the internal degrees of freedom of the electron are decoupled as the charge and spin degrees of freedom, while the elementary excitations are not quasi-particles but collective modes for the charge and spin degrees of freedom, i.e., the holon and spinon, then these holon and spinon might be responsible for the nonconventional behaviours. Many unusual properties of the underdoped cuprates are extensively studied following this line within the 2D  $t$ – $J$  type model [4, 16].

The decoupling of the charge and spin degrees of freedom of electron is undoubtedly correct in one-dimensional (1D) interacting electron systems [17], where the charge and spin degrees of freedom are represented by boson operators that describe the excitations of charge-density wave and spin-density wave, respectively. In particular, the typical behaviour of the non-FL, i.e., the absence of the quasiparticle propagation and CSS, has been demonstrated theoretically within the 1D  $t$ – $J$  model [18]. Moreover, the holon and spinon as the real elementary excitations in 1D cuprates have been observed directly by the ARPES experiment [19]. Therefore both theoretical and experimental studies indicate that the existence of the real holon and spinon is common in 1D [20]. However, the case in 2D is very complex since there are many competing degrees of freedom [1, 2]. As a consequence, both experimental investigation and theoretical understanding are extremely difficult [1–4]. Among the unusual properties of the underdoped cuprates, a hallmark is the charge transport [11–14], where the conductivity shows a non-Drude behaviour at low energies, and is carried by  $x$  holes, where  $x$  is the hole doping concentration, while the resistivity exhibits a linear temperature behaviour over a wide range of temperatures. This is a strong piece of experimental evidence supporting the notion of CSS, since not even conventional electron–electron scattering would show the striking linear rise of scattering rate above the Debye frequency, and if there is no CSS, the phonons should affect these properties [21]. Moreover, it has been argued that the most plausible source of the absence of phonon scattering and of pair-breaking effects seems to be CSS [21], and further, compelling evidence for CSS in doped cuprates has been found from the experimental test of the Wiedemann–Franz law, where a clear departure from the universal Wiedemann–Franz law for the typical FL behaviour is observed [22]. On the numerical study front, the crossover from the FL to non-FL behaviour with decreasing the hole doping concentration near the Mott transition has been found within the 2D  $t$ – $J$  model [23]. Furthermore, it has been shown within the 2D  $t$ – $t'$ – $J$  model by using the exact diagonalization method that there is a tendency of holes to generate nontrivial spin environments; this effect leads to a decoupling of the spin from the charge [24]. In this case, a formal theory with the gauge invariant holon and spinon, i.e., the issue of whether the holon and spinon are real, is centrally important [25]. In this paper, we propose a partial CSS fermion-spin theory, and show that if the local single occupancy constraint is treated properly, then the physical electron can be decoupled completely by introducing the dressed holon and spinon. These dressed holon and spinon are gauge invariant, i.e., they are real in 2D. As an application of this theory, we discuss the charge and spin dynamics of the underdoped cuprates within the  $t$ – $t'$ – $J$  model, and the results are qualitatively similar to that seen in experiments.

The paper is organized as follows. The framework of the partial CSS fermion-spin theory is presented in section 2. Within this theory, the single-particle dressed holon and spinon Green functions of the  $t$ – $t'$ – $J$  model are calculated in section 3 by considering the dressed holon–spinon interaction, where the dressed holon and spinon self-energies are obtained by using the equation of motion method. In section 4, we discuss the charge transport of the

underdoped cuprates. The incommensurate (IC) spin response of the underdoped cuprates is studied in section 5. Section 6 is devoted to a summary and discussions.

## 2. Gauge invariant dressed holon and spinon

We start from the  $t$ - $t'$ - $J$  model defined on a square lattice as [3, 26],

$$H = -t \sum_{i\hat{\eta}\sigma} C_{i\sigma}^\dagger C_{i+\hat{\eta}\sigma} + t' \sum_{i\hat{\tau}\sigma} C_{i\sigma}^\dagger C_{i+\hat{\tau}\sigma} + \mu \sum_{i\sigma} C_{i\sigma}^\dagger C_{i\sigma} + J \sum_{i\hat{\eta}} \mathbf{S}_i \cdot \mathbf{S}_{i+\hat{\eta}} \quad (1)$$

where  $\hat{\eta} = \pm\hat{x}, \pm\hat{y}$ ,  $\hat{\tau} = \pm\hat{x} \pm \hat{y}$ ,  $C_{i\sigma}^\dagger$  ( $C_{i\sigma}$ ) is the electron creation (annihilation) operator,  $\mathbf{S}_i = C_{i\sigma}^\dagger \vec{\sigma} C_{i\sigma}/2$  is spin operator with  $\vec{\sigma} = (\sigma_x, \sigma_y, \sigma_z)$  as Pauli matrices, and  $\mu$  is the chemical potential. The  $t$ - $t'$ - $J$  model (1) is subject to an important local constraint  $\sum_{\sigma} C_{i\sigma}^\dagger C_{i\sigma} \leq 1$  that a given site can not be occupied by more than one electron. In the  $t$ - $t'$ - $J$  model, the strong electron correlation manifests itself by this constraint, and therefore the crucial requirement is to impose this constraint [3, 26–28]. It has been shown that this constraint can be treated properly within the fermion-spin theory [29]. In this section, we show that the dressed holon and spinon in the fermion-spin theory are gauge invariant. Following the discussions in [29], we decouple the constrained electron operator as

$$C_{i\sigma} = h_i^\dagger a_{i\sigma}, \quad (2)$$

with the constraint  $\sum_{\sigma} a_{i\sigma}^\dagger a_{i\sigma} = 1$ , where the spinless fermion operator  $h_i$  keeps track of the charge degree of freedom, while the boson operator  $a_{i\sigma}$  keeps track of the spin degree of freedom. Then the Hamiltonian (1) can be rewritten as

$$H = -t \sum_{i\hat{\eta}\sigma} h_i a_{i\sigma}^\dagger h_{i+\hat{\eta}}^\dagger a_{i+\hat{\eta}\sigma} + t' \sum_{i\hat{\tau}\sigma} h_i a_{i\sigma}^\dagger h_{i+\hat{\tau}}^\dagger a_{i+\hat{\tau}\sigma} - \mu \sum_i h_i^\dagger h_i + J \sum_{i\hat{\eta}} (h_i h_i^\dagger) \mathbf{S}_i \cdot \mathbf{S}_{i+\hat{\eta}} (h_{i+\hat{\eta}} h_{i+\hat{\eta}}^\dagger), \quad (3)$$

where the pseudospin operator  $\mathbf{S}_i = a_i^\dagger \vec{\sigma} a_i/2$ . In this case, the electron constraint  $\sum_{\sigma} C_{i\sigma}^\dagger C_{i\sigma} = 1 - h_i^\dagger h_i \leq 1$  is exactly satisfied, with  $n_i^{(h)} = h_i^\dagger h_i$  is the holon number at site  $i$ , equal to 1 or 0. This decoupling scheme is called as the  $\text{CP}^1$  representation [30]. The advantage of this formalism is that the charge and spin degrees of freedom of the electron may be separated at the mean field (MF) level, where the elementary charge and spin excitations are called the holon and spinon, respectively. We call such holon and spinon as the *bare holon and spinon*, respectively, since an extra  $U(1)$  gauge degree of freedom related with the constraint  $\sum_{\sigma} a_{i\sigma}^\dagger a_{i\sigma} = 1$  appears, i.e., the  $\text{CP}^1$  representation is invariant under a local  $U(1)$  gauge transformation,

$$h_i \rightarrow h_i e^{i\theta_i}, \quad a_{i\sigma} \rightarrow a_{i\sigma} e^{i\theta_i}, \quad (4)$$

and then all physical quantities should be invariant with respect to this transformation. Thus both bare holon  $h_i$  and spinon  $a_{i\sigma}$  are not gauge invariant, and they are strongly coupled by these  $U(1)$  gauge field fluctuations. In other words, these bare holon and spinon are not real.

However, the constrained  $\text{CP}^1$  boson  $a_{i\sigma}$  can be mapped exactly onto the pseudospin representation defined with an additional phase factor; this is because the empty and doubly occupied spin states have been ruled out due to the constraint  $a_{i\uparrow}^\dagger a_{i\uparrow} + a_{i\downarrow}^\dagger a_{i\downarrow} = 1$ , and only the spin-up and spin-down singly occupied spin states are allowed, therefore the original four-dimensional representation space is reduced to a 2D space. Due to the symmetry of the spin-up and spin-down states,  $|\text{occupied}\rangle_\uparrow = \begin{pmatrix} 1 \\ 0 \end{pmatrix}_\uparrow$  and  $|\text{empty}\rangle_\uparrow = \begin{pmatrix} 0 \\ 1 \end{pmatrix}_\uparrow$  are singly-occupied and

empty spin-up, while  $|\text{occupied}\rangle_{\downarrow} = \begin{pmatrix} 0 \\ 1 \end{pmatrix}_{\downarrow}$  and  $|\text{empty}\rangle_{\downarrow} = \begin{pmatrix} 1 \\ 0 \end{pmatrix}_{\downarrow}$  are singly-occupied and empty spin-down states, respectively; thus the constrained  $\text{CP}^1$  boson operators  $a_{i\sigma}$  can be represented in this reduced 2D space as

$$a_{\uparrow} = e^{i\Phi_{\uparrow}} |\text{occupied}\rangle_{\downarrow} \langle \text{occupied}| = e^{i\Phi_{\uparrow}} \begin{pmatrix} 0 & 0 \\ 1 & 0 \end{pmatrix} = e^{i\Phi_{\uparrow}} S^{-}, \quad (5a)$$

$$a_{\downarrow} = e^{i\Phi_{\downarrow}} |\text{occupied}\rangle_{\uparrow} \langle \text{occupied}| = e^{i\Phi_{\downarrow}} \begin{pmatrix} 0 & 1 \\ 0 & 0 \end{pmatrix} = e^{i\Phi_{\downarrow}} S^{+}, \quad (5b)$$

where  $S^{-}$  is the  $S^z$  lowering operator, while  $S^{+}$  is the  $S^z$  raising operator; then the constraint  $\sum_{\sigma} a_{i\sigma}^{\dagger} a_{i\sigma} = S_i^{+} S_i^{-} + S_i^{-} S_i^{+} = 1$  is exactly satisfied. Obviously, the bare spinon contains both phase and amplitude parts, and the phase part is described by the phase factor  $e^{i\Phi_{i\sigma}}$ , while the amplitude part is described by the spin operator  $S_i$ . In this case, the electron decoupling form (2) with the constraint can be expressed as

$$C_{i\uparrow} = h_i^{\dagger} e^{i\Phi_{i\uparrow}} S_i^{-}, \quad C_{i\downarrow} = h_i^{\dagger} e^{i\Phi_{i\downarrow}} S_i^{+}, \quad (6)$$

with the local  $U(1)$  gauge transformation (4) rewritten as

$$h_i \rightarrow h_i e^{i\theta_i}, \quad \Phi_{i\sigma} \rightarrow \Phi_{i\sigma} + \theta_i. \quad (7)$$

Moreover, the phase factor of the bare spinon  $e^{i\Phi_{i\sigma}}$  can be incorporated into the bare holon; thus we obtain a new fermion-spin transformation from equation (6) as

$$C_{i\uparrow} = h_{i\uparrow}^{\dagger} S_i^{-}, \quad C_{i\downarrow} = h_{i\downarrow}^{\dagger} S_i^{+}, \quad (8)$$

where the *spinful fermion operator*  $h_{i\sigma} = e^{-i\Phi_{i\sigma}} h_i$  describes the charge degree of freedom together with the phase part of the spin degree of freedom (*dressed holon*), while the spin operator  $S_i$  describes the amplitude part of the spin degree of freedom (*dressed spinon*). This electron decoupling form (8) is called a partial CSS since only the amplitude part of the spin degree of freedom is separated from the electron operator. These dressed holon and spinon are invariant under the local  $U(1)$  gauge transformation (7), and therefore all physical quantities from the dressed holon and spinon also are invariant with respect to this gauge transformation. In this sense, the dressed holon and spinon are real. The dressed holon carries a spinon cloud (magnetic flux), and is a magnetic dressing [24]. In other words, the dressed holon carries some spinon messages, i.e., it shares some effects of spinon configuration rearrangements due to the presence of the hole itself. We emphasize that the dressed holon  $h_{i\sigma} = e^{-i\Phi_{i\sigma}} h_i$  is the spinless fermion  $h_i$  (bare holon) incorporated in the spinon cloud  $e^{-i\Phi_{i\sigma}}$  (magnetic flux). Although in the common sense  $h_{i\sigma}$  is not an real spinful fermion operator, it behaves like a spinful fermion. In correspondence with these special physical properties, we find that  $h_{i\sigma}^{\dagger} h_{i\sigma} = h_i^{\dagger} e^{i\Phi_{i\sigma}} e^{-i\Phi_{i\sigma}} h_i = h_i^{\dagger} h_i$ , which guarantees that the electron constraint,  $\sum_{\sigma} C_{i\sigma}^{\dagger} C_{i\sigma} = S_i^{+} h_{i\uparrow} h_{i\uparrow}^{\dagger} S_i^{-} + S_i^{-} h_{i\downarrow} h_{i\downarrow}^{\dagger} S_i^{+} = h_i h_i^{\dagger} (S_i^{+} S_i^{-} + S_i^{-} S_i^{+}) = 1 - h_i^{\dagger} h_i \leq 1$ , is always satisfied in analytical calculations. Moreover the double *spinful fermion* occupancy,  $h_{i\sigma}^{\dagger} h_{i-\sigma}^{\dagger} = e^{i\Phi_{i\sigma}} h_i^{\dagger} h_i^{\dagger} e^{i\Phi_{i-\sigma}} = 0$  and  $h_{i\sigma} h_{i-\sigma} = e^{-i\Phi_{i\sigma}} h_i h_i e^{-i\Phi_{i-\sigma}} = 0$ , is ruled out automatically. Since the spinless fermion  $h_i$  and spin operators  $S_i^{+}$  and  $S_i^{-}$  obey the anticommutation relation and Pauli spin algebra, respectively, it is then easy to show that the spinful fermion  $h_{i\sigma}$  also obeys the same anticommutation relation as the spinless fermion  $h_i$ .

Although the choice of the  $\text{CP}^1$  representation is convenient, so long as  $h_i^{\dagger} h_i = 1$ ,  $\sum_{\sigma} C_{i\sigma}^{\dagger} C_{i\sigma} = 0$ , no matter what the values of  $S_i^{+} S_i^{-}$  and  $S_i^{-} S_i^{+}$  are; therefore a ‘spin’ even to an empty site has been assigned. It has been shown [29] that this defect can be cured by introducing a projection operator  $P_i$ , i.e., the constrained electron operator can be mapped exactly using the fermion-spin transformation (8) defined with an additional projection operator  $P_i$ . However,

this projection operator is cumbersome to handle in the many cases, and it has been dropped in the actual calculations [29, 31]. It has been shown [29, 31, 32] that such treatment leads to errors of the order  $x$  in counting the number of spin states, which is negligible for small dopings. Moreover, the electron constraint is still exactly obeyed even in the MF approximation (MFA), and therefore the essential physics of the gauge invariant dressed holon and spinon is kept. This is because the constrained electron operator  $C_{i\sigma}$  in the  $t$ - $J$  type model can also be mapped onto the slave-fermion formalism [31] as  $C_{i\sigma} = h_i^\dagger b_{i\sigma}$  with the constraint  $h_i^\dagger h_i + \sum_\sigma b_{i\sigma}^\dagger b_{i\sigma} = 1$ . We can solve this constraint by rewriting the boson operators  $b_{i\sigma}$  in terms of the  $CP^1$  boson operators  $a_{i\sigma}$  as  $b_{i\sigma} = a_{i\sigma} \sqrt{1 - h_i^\dagger h_i}$  supplemented by the constraint  $\sum_\sigma a_{i\sigma}^\dagger a_{i\sigma} = 1$ . As mentioned above, the  $CP^1$  boson operators  $a_{i\uparrow}$  and  $a_{i\downarrow}$  with the constraint can be identified with the pseudospin lowering and raising operators, respectively, defined with the additional phase factor; therefore the projection operator is approximately related to the holon number operator by  $P_i \sim \sqrt{1 - h_{i\sigma}^\dagger h_{i\sigma}} = \sqrt{1 - h_i^\dagger h_i}$ , and its main role is to remove the spurious spin when there is a holon at the site  $i$ .

### 3. Dressed holon and spinon Green functions

Before discussing the charge and spin dynamics, let us first calculate the dressed holon and spinon Green functions. The low-energy behaviour of the  $t$ - $t'$ - $J$  model in the partial CSS fermion-spin representation can be expressed as [29, 31]

$$H = -t \sum_{i\hat{\eta}} (h_{i\uparrow} S_i^+ h_{i+\hat{\eta}\uparrow}^\dagger S_{i+\hat{\eta}}^- + h_{i\downarrow} S_i^- h_{i+\hat{\eta}\downarrow}^\dagger S_{i+\hat{\eta}}^+) + t' \sum_{i\hat{\tau}} (h_{i\uparrow} S_i^+ h_{i+\hat{\tau}\uparrow}^\dagger S_{i+\hat{\tau}}^- + h_{i\downarrow} S_i^- h_{i+\hat{\tau}\downarrow}^\dagger S_{i+\hat{\tau}}^+) - \mu \sum_{i\sigma} h_{i\sigma}^\dagger h_{i\sigma} + J_{\text{eff}} \sum_{i\hat{\eta}} \mathbf{S}_i \cdot \mathbf{S}_{i+\hat{\eta}}. \quad (9)$$

where  $J_{\text{eff}} = (1-x)^2 J$ , and  $x = \langle h_{i\sigma}^\dagger h_{i\sigma} \rangle = \langle h_i^\dagger h_i \rangle$  is the hole doping concentration. As a consequence, the kinetic part in the  $t$ - $t'$ - $J$  model has been expressed as the dressed holon-spinon interaction, which dominates the essential physics of the underdoped cuprates. The one-particle dressed holon and spinon two-time Green functions are defined as

$$g_\sigma(i-j, t-t') = -i\theta(t-t') \langle [h_{i\sigma}(t), h_{j\sigma}^\dagger(t')] \rangle = \langle \langle h_{i\sigma}(t); h_{j\sigma}^\dagger(t') \rangle \rangle, \quad (10a)$$

$$D(i-j, t-t') = -i\theta(t-t') \langle [S_i^+(t), S_j^-(t')] \rangle = \langle \langle S_i^+(t); S_j^-(t') \rangle \rangle, \quad (10b)$$

respectively, where  $\langle \dots \rangle$  is an average over the ensemble.

#### 3.1. Equation of motion

Since the dressed spinon operators obey Pauli algebra, our goal is to evaluate the dressed holon and spinon Green functions directly for the fermion and spin operators in terms of the equation of motion method. In the framework of the equation of motion, the time-Fourier transform of the two-time Green function  $G(\omega) = \langle \langle A; A^\dagger \rangle \rangle_\omega$  satisfies the equation [33]  $\omega \langle \langle A; A^\dagger \rangle \rangle_\omega = \langle [A, A^\dagger] \rangle + \langle \langle [A, H]; A^\dagger \rangle \rangle_\omega$ . If we define the orthogonal operator  $L$  as  $[A, H] = \zeta A - iL$  with  $\langle [L, A^\dagger] \rangle = 0$ , the full Green function can be expressed as

$$G(\omega) = G^{(0)}(\omega) + \frac{1}{\zeta^2} G^{(0)}(\omega) \langle \langle L; L^\dagger \rangle \rangle_\omega G^{(0)}(\omega), \quad (11)$$

where  $\zeta = \langle [A, A^\dagger] \rangle$ , and the MF Green function  $G^{(0)-1}(\omega) = (\omega - \zeta)/\zeta$ . It has been shown [33] that if the self-energy  $\Sigma(\omega)$  is identified as the irreducible part of  $\langle \langle L; L^\dagger \rangle \rangle_\omega$ , the

full Green function (11) can be evaluated as

$$G(\omega) = \frac{\zeta}{\omega - \zeta - \Sigma(\omega)}, \quad (12)$$

with  $\Sigma(\omega) = \langle\langle L; L^\dagger \rangle\rangle_\omega^{\text{irr}}/\zeta$ . In the framework of the diagrammatic technique,  $\Sigma(\omega)$  corresponds to the contribution of irreducible diagrams.

### 3.2. The mean-field theory

Within MFA, the  $t$ - $t'$ - $J$  model (9) can be decoupled as

$$H_{\text{MFA}} = H_t + H_J - 8Nt\chi_1\phi_1 + 8Nt'\chi_2\phi_2, \quad (13a)$$

$$H_t = \chi_1t \sum_{i\hat{\eta}\sigma} h_{i+\hat{\eta}\sigma}^\dagger h_{i\sigma} - \chi_2t' \sum_{i\hat{\tau}\sigma} h_{i+\hat{\tau}\sigma}^\dagger h_{i\sigma} - \mu \sum_{i\sigma} h_{i\sigma}^\dagger h_{i\sigma}, \quad (13b)$$

$$H_J = J_{\text{eff}} \sum_{i\hat{\eta}} [\frac{1}{2}\epsilon(S_i^+ S_{i+\hat{\eta}}^- + S_i^- S_{i+\hat{\eta}}^+) + S_i^Z S_{i+\hat{\eta}}^Z] - \phi_2t' \sum_{i\hat{\tau}} (S_i^+ S_{i+\hat{\tau}}^- + S_i^- S_{i+\hat{\tau}}^+), \quad (13c)$$

where the dressed holon's particle-hole parameters  $\phi_1 = \langle h_{i\sigma}^\dagger h_{i+\hat{\eta}\sigma} \rangle$  and  $\phi_2 = \langle h_{i\sigma}^\dagger h_{i+\hat{\tau}\sigma} \rangle$ , the dressed spinon correlation functions  $\chi_1 = \langle S_i^+ S_{i+\hat{\eta}}^- \rangle$  and  $\chi_2 = \langle S_i^+ S_{i+\hat{\tau}}^- \rangle$ , and  $\epsilon = 1 + 2t\phi_1/J_{\text{eff}}$ . Since AFLRO in the undoped cuprates is destroyed [34] by hole doping of the order  $\sim 0.024$ , there is therefore no AFLRO in the doped regime  $x \geq 0.025$ , i.e.,  $\langle S_i^z \rangle = 0$ , and a disordered spin liquid state emerges. It has been argued that this spin liquid state may play a crucial role in the mechanism for HTSC [3, 4]. In this paper, we focus on the normal-state properties in the doped regime without AFLRO. In this case, a similar MF theory [35] of the  $t$ - $J$  model based on the fermion-spin theory has been discussed within the Kondo-Yamaji decoupling scheme [36], which is a stage one step further than the Tyablikov's decoupling scheme [37]. In this MF theory [35], the phase factor  $e^{i\Phi_{i\sigma}}$  describing the phase part of the spin degree of freedom was not considered. Following their discussions [35], we obtain the MF dressed holon and spinon Green functions in the present case as

$$g_\sigma^{(0)}(\mathbf{k}, \omega) = \frac{1}{\omega - \xi_{\mathbf{k}}}, \quad (14a)$$

$$D^{(0)}(\mathbf{k}, \omega) = \frac{B_{\mathbf{k}}}{\omega^2 - \omega_{\mathbf{k}}^2}, \quad (14b)$$

respectively, where  $B_{\mathbf{k}} = \lambda_1[2\chi_1^z(\epsilon\gamma_{\mathbf{k}} - 1) + \chi_1(\gamma_{\mathbf{k}} - \epsilon)] - \lambda_2(2\chi_2^z\gamma_{\mathbf{k}}' - \chi_2)$ ,  $\lambda_1 = 2ZJ_{\text{eff}}$ ,  $\lambda_2 = 4Z\phi_2t'$ ,  $\gamma_{\mathbf{k}} = (1/Z) \sum_{\hat{\eta}} e^{i\mathbf{k}\cdot\hat{\eta}}$ ,  $\gamma_{\mathbf{k}}' = (1/Z) \sum_{\hat{\tau}} e^{i\mathbf{k}\cdot\hat{\tau}}$ ,  $Z$  is the number of the nearest neighbour or second-nearest neighbour sites, and the MF dressed holon and spinon excitation spectra are given by

$$\xi_{\mathbf{k}} = Zt\chi_1\gamma_{\mathbf{k}} - Zt'\chi_2\gamma_{\mathbf{k}}' - \mu, \quad (15a)$$

$$\omega_{\mathbf{k}}^2 = A_1(\gamma_{\mathbf{k}})^2 + A_2(\gamma_{\mathbf{k}}')^2 + A_3\gamma_{\mathbf{k}}\gamma_{\mathbf{k}}' + A_4\gamma_{\mathbf{k}} + A_5\gamma_{\mathbf{k}}' + A_6, \quad (15b)$$

respectively, with  $A_1 = \alpha\epsilon\lambda_1^2(\epsilon\chi_1^z + \chi_1/2)$ ,  $A_2 = \alpha\lambda_2^2\chi_2^z$ ,  $A_3 = -\alpha\lambda_1\lambda_2(\epsilon\chi_1^z + \epsilon\chi_2^z + \chi_1/2)$ ,  $A_4 = -\epsilon\lambda_1^2[\alpha(\chi_1^z + \epsilon\chi_1/2) + (\alpha C_1^z + (1-\alpha)/(4Z) - \alpha\epsilon\chi_1/(2Z)) + (\alpha C_1 + (1-\alpha)/(2Z) - \alpha\chi_1^z/2)/2] + \alpha\lambda_1\lambda_2(C_3 + \epsilon\chi_2)/2$ ,  $A_5 = -3\alpha\lambda_2^2\chi_2/(2Z) + \alpha\lambda_1\lambda_2(\chi_1^z + \epsilon\chi_1/2 + C_3^z)$ ,  $A_6 = \lambda_1^2[\alpha C_1^z + (1-\alpha)/(4Z) - \alpha\epsilon\chi_1/(2Z) + \epsilon^2(\alpha C_1 + (1-\alpha)/(2Z) - \alpha\chi_1^z/2)/2] + \lambda_2^2(\alpha C_2 + (1-\alpha)/(2Z) - \alpha\chi_2^z/2)/2 - \alpha\epsilon\lambda_1\lambda_2 C_3$ , and the spinon correlation functions  $\chi_1^z = \langle S_i^z S_{i+\hat{\eta}}^z \rangle$ ,  $\chi_2^z = \langle S_i^z S_{i+\hat{\tau}}^z \rangle$ ,  $C_1 = (1/Z^2) \sum_{\hat{\eta}, \hat{\eta}'} \langle S_{i+\hat{\eta}}^+ S_{i+\hat{\eta}'}^- \rangle$ ,  $C_1^z = (1/Z^2) \sum_{\hat{\eta}, \hat{\eta}'} \langle S_{i+\hat{\eta}}^z S_{i+\hat{\eta}'}^z \rangle$ ,  $C_2 = (1/Z^2) \sum_{\hat{\tau}, \hat{\tau}'} \langle S_{i+\hat{\tau}}^+ S_{i+\hat{\tau}'}^- \rangle$ ,  $C_3 = (1/Z) \sum_{\hat{\tau}} \langle S_{i+\hat{\eta}}^+ S_{i+\hat{\tau}}^- \rangle$ , and  $C_3^z = (1/Z) \sum_{\hat{\tau}} \langle S_{i+\hat{\eta}}^z S_{i+\hat{\tau}}^z \rangle$ . In order not to violate the sum rule of the correlation function  $\langle S_i^+ S_i^- \rangle = 1/2$  in the case without AFLRO, the important decoupling parameter  $\alpha$  has been introduced in the MF

calculation [35, 36], which can be regarded as the vertex correction. All the above MF order parameters, decoupling parameter  $\alpha$ , and chemical potential  $\mu$  are determined by the self-consistent calculation [35].

### 3.3. The dressed holon and spinon self-energies

With the help of equation (12), the full dressed holon and spinon Green functions of the  $t$ - $t'$ - $J$  model (9) are expressed as

$$g_\sigma(\mathbf{k}, \omega) = \frac{1}{\omega - \xi_k - \Sigma_h^{(2)}(\mathbf{k}, \omega)}, \quad (16a)$$

$$D(\mathbf{k}, \omega) = \frac{B_k}{\omega^2 - \omega_k^2 - \Sigma_s^{(2)}(\mathbf{k}, \omega)}, \quad (16b)$$

respectively, where the second-order dressed holon self-energy from the dressed spinon pair bubble  $\Sigma_h^{(2)}(\mathbf{k}, \omega) = \langle \langle L_k^{(h)}(t); L_k^{(h)\dagger}(t') \rangle \rangle_\omega$  with the orthogonal operator  $L_i^{(h)} = -t \sum_{\hat{\eta}} h_{i+\hat{\eta}\sigma} (S_{i+\hat{\eta}}^- S_i^+ - \chi_1) + t' \sum_{\hat{\tau}} h_{i+\hat{\tau}\sigma} (S_{i+\hat{\tau}}^- S_i^+ - \chi_2)$ , and can be evaluated as [31]

$$\begin{aligned} \Sigma_h^{(2)}(\mathbf{k}, \omega) = & \frac{1}{2} \left( \frac{Z}{N} \right)^2 \sum_{pp'} \gamma_{12}^2(\mathbf{k}, \mathbf{p}, \mathbf{p}') \frac{B_{p'} B_{p+p'}}{4\omega_{p'} \omega_{p+p'}} \left( \frac{F_1^{(h)}(k, p, p')}{\omega + \omega_{p+p'} - \omega_{p'} - \xi_{p+k}} \right. \\ & + \frac{F_2^{(h)}(k, p, p')}{\omega + \omega_{p'} - \omega_{p+p'} - \xi_{p+k}} + \frac{F_3^{(h)}(k, p, p')}{\omega + \omega_{p'} + \omega_{p+p'} - \xi_{p+k}} \\ & \left. - \frac{F_4^{(h)}(k, p, p')}{\omega - \omega_{p+p'} - \omega_{p'} - \xi_{p+k}} \right), \quad (17) \end{aligned}$$

where  $\gamma_{12}^2(\mathbf{k}, \mathbf{p}, \mathbf{p}') = [(t\gamma_{p'+p+k} - t'\gamma_{p'+p+k}^2) + (t\gamma_{p'-k} - t'\gamma_{p'-k}^2)]$ ,  $F_1^{(h)}(k, p, p') = n_F(\xi_{p+k}) [n_B(\omega_{p'}) - n_B(\omega_{p+p'})] + n_B(\omega_{p+p'})[1 + n_B(\omega_{p'})]$ ,  $F_2^{(h)}(k, p, p') = n_F(\xi_{p+k}) [n_B(\omega_{p+p'}) - n_B(\omega_{p'})] + n_B(\omega_{p'})[1 + n_B(\omega_{p+p'})]$ ,  $F_3^{(h)}(k, p, p') = n_F(\xi_{p+k}) [1 + n_B(\omega_{p+p'}) + n_B(\omega_{p'})] + n_B(\omega_{p'})n_B(\omega_{p+p'})$ ,  $F_4^{(h)}(k, p, p') = n_F(\xi_{p+k}) [1 + n_B(\omega_{p+p'}) + n_B(\omega_{p'})] - [1 + n_B(\omega_{p'})][1 + n_B(\omega_{p+p'})]$ , and  $n_B(\omega_p)$  and  $n_F(\xi_p)$  are the boson and fermion distribution functions, respectively. This dressed holon self-energy is ascribed purely to the dressed holon–spinon interaction, and characterizes the competition between the kinetic energy and magnetic energy. The calculation of the dressed spinon self-energy is quite tedious [38], since our starting point is the dressed spinon MF solution [35] within the Kondo–Yamaji decoupling scheme in section 3.2. From equation (11) and the MF dressed spinon Green function (14b), the full dressed spinon Green function satisfies the relation [38],  $\omega^2 D(k, \omega) = B_k + \langle \langle [S_i^+(t), H(t)], H(t); S_j^-(t') \rangle \rangle_{k, \omega}$  with  $[[S_i^+, H], H]_k = \omega_k^2 S_k^+ - i\Gamma_k^{(s)}$ . In the disordered liquid state without AFLRO, the dressed holon–spinon interaction should dominate the essential physics [38]. In this case, the orthogonal operator  $L_k^{(s)}$  for the dressed spinon can be selected from  $\Gamma_k^{(s)}$  as [38]

$$\begin{aligned} L_i^{(s)} = & -(2\epsilon\chi_1^z + \chi_1)\lambda_1 \frac{1}{Z} \sum_{\hat{\eta}, \hat{a}} t_{\hat{a}} (h_{i+\hat{\eta}\uparrow}^\dagger h_{i+\hat{\eta}+\hat{a}\uparrow} + h_{i+\hat{\eta}+\hat{a}\downarrow}^\dagger h_{i+\hat{\eta}\downarrow} - 2\phi_{\hat{a}}) S_{i+\hat{\eta}+\hat{a}}^+ \\ & + [(2\chi_1^z + \epsilon\chi_1)\lambda_1 - \chi_2\lambda_2] \sum_{\hat{a}} t_{\hat{a}} (h_{i\uparrow}^\dagger h_{i+\hat{a}\uparrow} + h_{i+\hat{a}\downarrow}^\dagger h_{i\downarrow} - 2\phi_{\hat{a}}) S_{i+\hat{a}}^+ \\ & + 2\chi_2^z\lambda_2 \frac{1}{Z} \sum_{\hat{\tau}, \hat{a}} t_{\hat{a}} (h_{i+\hat{\tau}\uparrow}^\dagger h_{i+\hat{\tau}+\hat{a}\uparrow} + h_{i+\hat{\tau}+\hat{a}\downarrow}^\dagger h_{i+\hat{\tau}\downarrow} - 2\phi_{\hat{a}}) S_{i+\hat{\tau}+\hat{a}}^+, \quad (18) \end{aligned}$$



where  $\hat{a} = \hat{\eta}, \hat{\tau}$ , with  $t_{\hat{\eta}} = t, \phi_{\hat{\eta}} = \phi_1$ , and  $t_{\hat{\tau}} = -t', \phi_{\hat{\tau}} = \phi_2$ . Following [38], we obtain the dressed spinon self-energy  $\Sigma_s^{(2)}(\mathbf{k}, \omega) = \langle\langle L_i^{(s)}(t); L_j^{(s)\dagger}(t') \rangle\rangle_{k,\omega}$ ,

$$\Sigma_s^{(2)}(\mathbf{k}, \omega) = B_k \left( \frac{Z}{N} \right)^2 \sum_{pp'} \gamma_{12}^2(\mathbf{k}, \mathbf{p}, \mathbf{p}') \frac{B_{k+p}}{2\omega_{k+p}} \times \left( \frac{F_1^{(s)}(k, p, p')}{\omega + \xi_{p+p'} - \xi_{p'} - \omega_{k+p}} - \frac{F_2^{(s)}(k, p, p')}{\omega + \xi_{p+p'} - \xi_{p'} + \omega_{k+p}} \right), \quad (19)$$

with  $F_1^{(s)}(k, p, p') = n_F(\xi_{p+p'})[1 - n_F(\xi_{p'})] - n_B(\omega_{k+p})[n_F(\xi_{p'}) - n_F(\xi_{p+p'})]$ , and  $F_2^{(s)}(k, p, p') = n_F(\xi_{p+p'})[1 - n_F(\xi_{p'})] + [1 + n_B(\omega_{k+p})][n_F(\xi_{p'}) - n_F(\xi_{p+p'})]$ . Within the diagrammatic technique, this dressed spinon self-energy  $\Sigma_s^{(2)}(\mathbf{k}, \omega)$  corresponds to the contribution from the dressed holon pair bubble, and is consistent with our previous result [38].

#### 4. Charge transport

Recently, the emergence and evolution of metallic transport in doped cuprates have been extensively studied by virtue of systematic transport measurements [14]. It is shown that the resistivity shows a crossover from low temperature insulating-like to moderate temperature metallic-like behaviour in the heavily underdoped regime ( $0.025 \leq x < 0.055$ ), and a temperature linear dependence with deviations at low temperatures in the underdoped regime ( $0.055 < x < 0.15$ ). These striking behaviours have been found to be intriguingly related to the AF correlation [14]. In this case, a natural question is what is the physical origin of this transport transformation from the insulating liquid state in the heavily underdoped regime to the unusual metallic state in the underdoped regime? In this section, we try to discuss this issue. Since the local constraint has been treated properly in the partial CSS fermion-spin theory, the extra  $U(1)$  gauge degree of freedom related with the local constraint is incorporated into the dressed holon as mentioned in section 2. In this case, the external electronic field only is coupled to the dressed holons, and the conductivity is given by

$$\sigma(\omega) = -\frac{\text{Im } \Pi_h(\omega)}{\omega}, \quad (20)$$

where  $\Pi_h(\omega)$  is the dressed holon current-current correlation function, and is defined as  $\Pi_h(t - t') = \langle\langle j_h(t) j_h(t') \rangle\rangle$ , where the current density of the dressed holons is obtained by taking the time derivation of the polarization operator with the use of the equation of motion as [31]  $j_h = (e\chi_1 t/2) \sum_{i\hat{\eta}\sigma} \hat{\eta} h_{i+\hat{\eta}\sigma}^\dagger h_{i\sigma} - (e\chi_2 t'/2) \sum_{i\hat{\tau}\sigma} \hat{\tau} h_{i+\hat{\tau}\sigma}^\dagger h_{i\sigma}$ . With the help of the full dressed holon Green function (16a), the current-current correlation function is evaluated as

$$\Pi_h(i\omega_n) = -\left( \frac{Ze}{2} \right)^2 \frac{1}{N} \sum_k \gamma_s^2(\mathbf{k}) \frac{1}{\beta} \sum_{i\omega'_m\sigma} g_\sigma(\mathbf{k}, i\omega'_m + i\omega_n) g_\sigma(\mathbf{k}, i\omega'_m), \quad (21)$$

where  $i\omega_n$  is the Matsubara frequency,  $\gamma_s^2(\mathbf{k}) = [\sin^2 k_x (\chi_1 t - 2\chi_2 t' \cos k_y)^2 + \sin^2 k_y (\chi_1 t - 2\chi_2 t' \cos k_x)^2]/4$ . The full dressed holon Green function can be expressed as frequency integrals in terms of the spectral representation,

$$g_\sigma(\mathbf{k}, i\omega_n) = \int_{-\infty}^{\infty} \frac{d\omega}{2\pi} \frac{A_\sigma^{(h)}(\mathbf{k}, \omega)}{i\omega_n - \omega}, \quad (22)$$

with the dressed holon spectral function  $A_\sigma^{(h)}(\mathbf{k}, \omega) = -2 \text{Im } g_\sigma(\mathbf{k}, \omega)$ . Substituting the equations (22) and (21) into equation (20), and evaluating the frequency summation, we obtain the conductivity as [31]

$$\sigma(\omega) = \left( \frac{Ze}{2} \right)^2 \frac{1}{N} \sum_{k\sigma} \gamma_s^2(\mathbf{k}) \int_{-\infty}^{\infty} \frac{d\omega'}{2\pi} A_\sigma^{(h)}(\mathbf{k}, \omega' + \omega) A_\sigma^{(h)}(\mathbf{k}, \omega') \frac{n_F(\omega' + \omega) - n_F(\omega')}{\omega}. \quad (23)$$

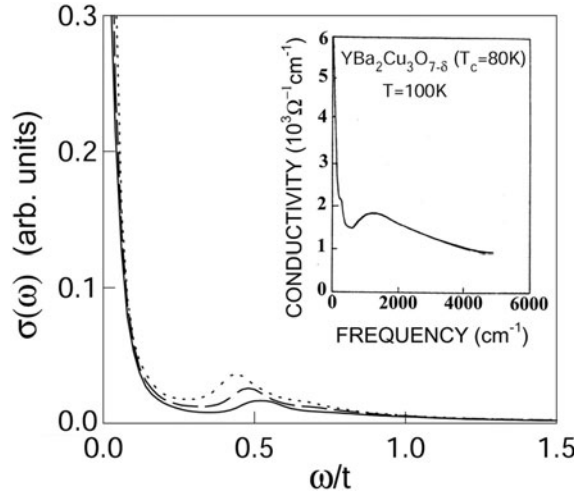


**Figure 1.** The conductivity at  $x = 0.03$  (solid curve),  $x = 0.05$  (dashed curve), and  $x = 0.07$  (dotted curve) with  $t/J = 2.5$  and  $t'/t = 0.15$  in  $T = 0$ . Inset: the experimental result of  $\text{YBa}_2\text{Cu}_3\text{O}_{7-x}$  taken from [11].

We have performed a numerical calculation for  $\sigma(\omega)$ , and the results at  $x = 0.03$  (solid curve),  $x = 0.05$  (dashed curve), and  $x = 0.07$  (dotted curve) for  $t/J = 2.5$  and  $t'/t = 0.15$  with  $T = 0$  are plotted in figure 1; hereinafter the charge  $e$  is set as the unit. For a comparison, the experimental result [11] of  $\text{YBa}_2\text{Cu}_3\text{O}_{7-x}$  is also plotted in figure 1 (inset). Our results show that there is a low-energy peak at  $\omega < 0.3t$  separated by a gap or pseudogap at  $0.3t$  from a midinfrared band. This midinfrared band is doping dependent: the component increases with increasing dopings for  $0.3t < \omega < 1.0t$  and is nearly independent of dopings for  $\omega > 1.0t$ ; however, the position of the midinfrared peak is shifted to lower energies with increased dopings. This reflects an increase in the mobile carrier density, and indicates that the spectral weight of the midinfrared sideband is taken from the Drude absorption; then the spectral weight from both low energy peak and midinfrared band represent the actual free-carrier density. For a better understanding of the optical properties, we have made a series of calculations for  $\sigma(\omega)$  at different temperatures, and the results at  $x = 0.06$  with  $T = 0$  (solid curve),  $T = 0.1J$  (dashed curve), and  $T = 0.3J$  (dotted curve) for  $t/J = 2.5$  and  $t'/t = 0.15$  are plotted in figure 2 in comparison with the experimental data [11] taken from  $\text{YBa}_2\text{Cu}_3\text{O}_{7-x}$  (inset). It is shown that  $\sigma(\omega)$  is temperature dependent for  $\omega < 1.0t$ , and almost temperature independent for  $\omega > 1.0t$ . The peak at low energies broadens and decreases in height with increasing temperatures, while the component in the low energy region increases with increasing temperatures, then there is a tendency towards the Drude-like behaviour. The midinfrared band is severely suppressed with increasing temperatures, and vanishes at high temperatures, in qualitative agreement with experiments [11, 12].

Now we turn to discuss the resistivity, which is evaluated as  $\rho = 1/\sigma_{\text{dc}}$ , with the dc conductivity  $\sigma_{\text{dc}}$  obtained from equation (23) as  $\sigma_{\text{dc}} = \lim_{\omega \rightarrow 0} \sigma(\omega)$ . This resistivity has been evaluated numerically, and the results are plotted in figure 3 as a function of temperature at  $x = 0.03$  (solid curve),  $x = 0.04$  (dashed curve),  $x = 0.05$  (dotted curve), and  $x = 0.06$  (chain curve) for  $t/J = 2.5$  and  $t'/t = 0.15$  in comparison with the experimental data [14] taken from  $\text{La}_{2-x}\text{Sr}_x\text{CuO}_4$  (inset). Our results show obviously that the resistivity is characterized by a crossover from the moderate temperature metallic-like to low temperature insulating-

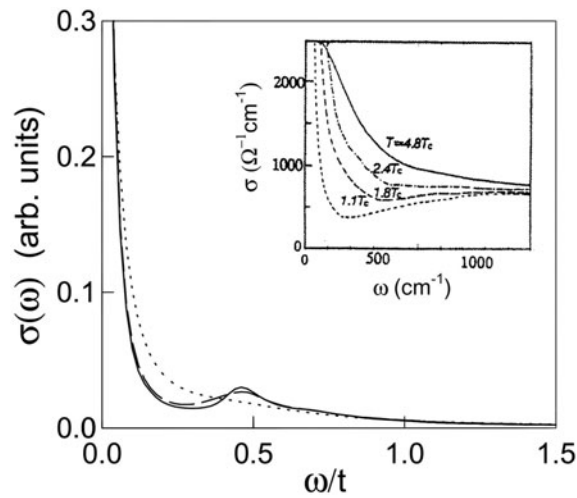


**Figure 2.** The conductivity at  $x = 0.06$  in  $T = 0$  (solid curve),  $T = 0.1J$  (dashed curve), and  $T = 0.3J$  (dotted curve) with  $t/J = 2.5$  and  $t'/t = 0.15$ . Inset: the experimental result of  $\text{YBa}_2\text{Cu}_3\text{O}_{7-x}$  taken from [11].

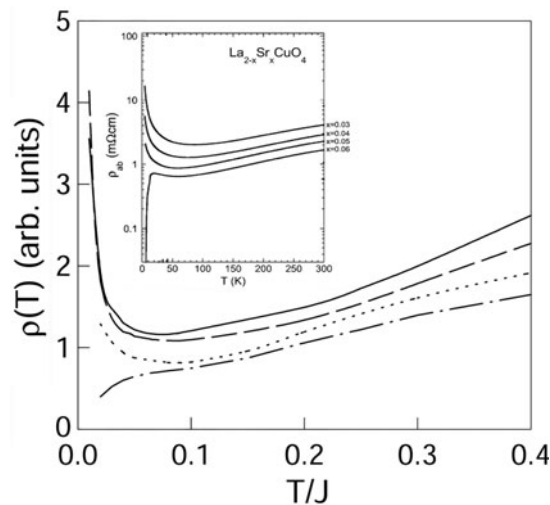


**Figure 3.** The electron resistivity as a function of temperature at  $x = 0.03$  (solid curve),  $x = 0.04$  (dashed curve),  $x = 0.05$  (dotted curve), and  $x = 0.06$  (chain curve) with  $t/J = 2.5$  and  $t'/t = 0.15$ . Inset: the experimental result of  $\text{La}_{2-x}\text{Sr}_x\text{CuO}_4$  taken from [14].

like behaviour in the heavily underdoped regime, and a temperature linear dependence with deviations at low temperatures in the underdoped regime. But even in the heavily underdoped regime, the resistivity exhibits metallic-like behaviour over a wide range of temperatures, which also is in qualitative agreement with experiments [14].

The perovskite parent compound of doped cuprates is a Mott insulator; when holes are doped into this insulator, there is a gain in the kinetic energy per hole proportional to  $t$  due to hopping, but at the same time, the spin correlation is destroyed, costing an energy of approximately  $J$  per site. Thus doped holes in a Mott insulator can be considered as a

competition between the kinetic energy ( $xt$ ) and magnetic energy ( $J$ ). The magnetic energy  $J$  favours the magnetic order for spins and results in frustration of the kinetic energy, while the kinetic energy  $xt$  favours delocalization of holes and tends to destroy the magnetic order. In the present partial CSS fermion-spin theory, the scattering of dressed holons dominates the charge transport, since the scattering rate is obtained from the dressed holon self-energy  $\Sigma_h^{(2)}(\mathbf{k}, \omega)$ , while this self-energy is evaluated by considering the dressed holon–spinon interaction, and characterizes a competition between the kinetic energy and magnetic energy. In this case, the striking behaviour in the resistivity is intriguingly related to this competition. In the heavily underdoped regime, the dressed holon kinetic energy is much smaller than the dressed spinon magnetic energy at lower temperatures due to the strong AF correlation, where the dressed holons are localized, and the scattering rate from the dressed holon self-energy is severely reduced; this leads to the insulating-like behaviour in the resistivity. With increasing temperatures, the dressed holon kinetic energy is increased, while the dressed spinon magnetic energy is decreased. In the region where the dressed holon kinetic energy is larger than the dressed spinon magnetic energy at moderate temperatures, the dressed holons can move in the background of the dressed spinon fluctuation; then the dressed holon scattering would give rise to the metallic-like behaviour in the resistivity. Since the charge transport is governed by the dressed holon scattering, the  $x$  dressed holons are responsible for the electron conductivity.

## 5. Incommensurate spin dynamics

The interplay between AF correlation and HTSC in doped cuprates is now well-established [1], but its full understanding is still a challenging issue. Experimentally, NMR, NQR, and  $\mu$ SR techniques, particularly inelastic neutron scattering, can provide rather detailed information on the spin dynamics of doped cuprates [5–10]. It has been shown [7, 8] that when AFLRO is suppressed, the IC magnetic correlation develops at a quartet of wavevector  $[\pi(1 \pm \delta), \pi]$  and  $[\pi, (1 \pm \delta)\pi]$ , where the incommensurability  $\delta$  increases almost linearly with the hole doping concentration  $x$  at lower dopings, and saturates at higher dopings. These exotic features are fully confirmed by the data both on the normal and superconducting states [7, 8]. It has been argued that the emergence of the IC magnetic correlation is due to dopings [39]. Although a sharp resonance peak at the commensurate AF wavevector has been observed in some optimally doped samples, this commensurate scattering is the main new feature that appears in the superconducting phase [40, 8]. In this section, we only discuss the IC magnetic correlation in the normal state. Within the present partial CSS fermion-spin theory, the spin fluctuation couples only to the dressed spinons; then the dynamical spin structure factor (DSSF) is obtained in terms of the full dressed spinon Green function (16b) as [38]

$$S(\mathbf{k}, \omega) = -2[1 + n_B(\omega)] \text{Im} D(k, \omega) \\ = -2[1 + n_B(\omega)] \frac{B_k \text{Im} \Sigma_s^{(2)}(\mathbf{k}, \omega)}{[\omega^2 - \omega_k^2 - \text{Re} \Sigma_s^{(2)}(\mathbf{k}, \omega)]^2 + [\text{Im} \Sigma_s^{(2)}(\mathbf{k}, \omega)]^2}, \quad (24)$$

where  $\text{Im} \Sigma_s^{(2)}(\mathbf{k}, \omega)$  and  $\text{Re} \Sigma_s^{(2)}(\mathbf{k}, \omega)$  are the corresponding imaginary part and real part of the dressed spinon self-energy function  $\Sigma_s^{(2)}(\mathbf{k}, \omega)$  in equation (19).

At the half-filling, the spin fluctuation scattering remains commensurate at the AF wavevector  $\mathbf{Q} = [1/2, 1/2]$  position (hereafter we use units of  $[2\pi, 2\pi]$ ), which is not presented here for the sake of space. Instead, we plot the DSSF spectrum  $S(\mathbf{k}, \omega)$  in the  $(k_x, k_y)$  plane at  $x = 0.06$  with  $T = 0.05J$  and  $\omega = 0.05J$  for  $t/J = 2.5$  and  $t'/t = 0.15$  in figure 4. This result shows that with dopings, there is a commensurate–IC transition in the spin fluctuation geometry, where all IC peaks lie on a circle of radius of  $\delta$ . Although some IC satellite diagonal

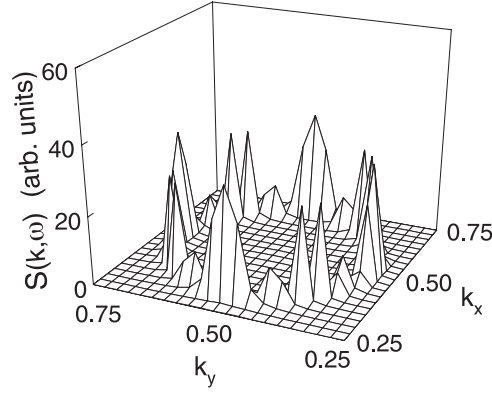


**Figure 4.** The dynamical spin structure factor spectrum in the  $(k_x, k_y)$  plane at  $x = 0.06$  in  $T = 0.05J$  and  $\omega = 0.05J$  with  $t/J = 2.5$  and  $t'/t = 0.15$ .

peaks appear, the main weight of the IC peaks is in the parallel direction, and these parallel peaks are located at  $[(1 \pm \delta)/2, 1/2]$  and  $[1/2, (1 \pm \delta)/2]$ . The IC peaks are very sharp at low temperatures and energies, which means that these low energy excitations have a dynamical coherence length at low temperatures that is larger than the instantaneous correlation length. For considering IC magnetic fluctuation at a relatively high energy, we have made a series of scans for  $S(\mathbf{k}, \omega)$  with several energies, and the result at  $x = 0.06$  in  $t/J = 2.5$  and  $t'/t = 0.15$  with  $T = 0.05J$  for  $\omega = 0.1J$  is shown in figure 5. Comparing it with figure 4 for the same set of parameters except for  $\omega = 0.05J$ , we see that at low temperatures, although the positions of the IC peaks are energy independent, the IC peaks broaden and weaken in amplitude as the energy increase, and vanish at high energies. This reflects that the excitation width increases with increasing energies, and thus leads to the lifetime of the excitations decreasing quickly with increasing energies. The present DSSF spectrum has been used to extract the doping dependence of the incommensurability  $\delta(x)$ , which is defined as the deviation of the peak position from the AF wavevector position, and the result is plotted in figure 6 in comparison with the experimental result [7] taken from  $\text{La}_{2-x}\text{Sr}_x\text{CuO}_4$  (inset). Our result shows that  $\delta(x)$  increases progressively with the doping concentration at lower dopings, but saturates at higher dopings, in qualitative agreement with experiments [7, 8].

The universal integrated dynamical spin response is a characteristic feature, and is closely related to many other normal-state properties [1]. The integrated dynamical spin response is manifested by the integrated dynamical spin susceptibility (IDSS), and is expressed as

$$I(\omega, T) = \frac{1}{N} \sum_{\mathbf{k}} \chi''(\mathbf{k}, \omega), \quad (25)$$

where the dynamical spin susceptibility is related to DSSF by the fluctuation dissipation theorem as  $\chi''(\mathbf{k}, \omega) = (1 - e^{-\beta\omega})S(\mathbf{k}, \omega) = -2 \text{Im} D(\mathbf{k}, \omega)$ . This IDSS has been evaluated numerically, and the results at  $x = 0.12$  for  $t/J = 2.5$  and  $t'/t = 0.15$  with  $T = 0.2J$  (solid curve),  $T = 0.3J$  (dashed curve), and  $T = 0.5J$  (dotted curve) are plotted in figure 7 in comparison with the experimental data [9] taken from  $\text{La}_{2-x}\text{Sr}_x\text{CuO}_4$  (inset). It is shown that the shape of the IDSS appears to be particularly universal, and can be scaled approximately as  $I(\omega, T) \propto \arctan[a_1\omega/T + a_3(\omega/T)^3]$ , where  $I(\omega, T)$  is almost constant for  $\omega/T > 1$ , and then begins to decrease with decreasing  $\omega/T$  for  $\omega/T < 1$ , also in qualitative agreement with experiments [9, 10].

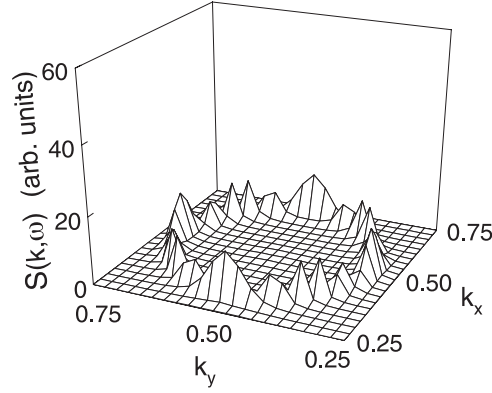


**Figure 5.** The dynamical spin structure factor spectrum in the  $(k_x, k_y)$  plane at  $x = 0.06$  with  $t/J = 2.5$  and  $t'/t = 0.15$  in  $T = 0.05J$  and  $\omega = 0.1J$ .

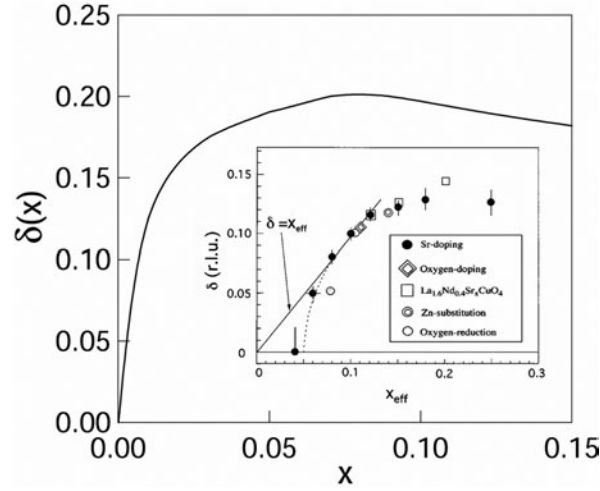


**Figure 6.** The doping dependence of the incommensurability  $\delta(x)$ . Inset: the experimental result for  $\text{La}_{2-x}\text{Sr}_x\text{CuO}_4$  taken from [7].

Although the scattering of the dressed spinons dominates the spin dynamics, the effect of the dressed holons on the dressed spinon part is critical in determining the characteristic feature of the IC magnetic correlation, which can be understood from the properties of the dressed spinon excitation spectrum  $E_k^2 = \omega_k^2 + \text{Re} \Sigma_s^{(2)}(\mathbf{k}, E_k)$ . During the calculation of the DSSF spectrum in equation (24), we find when  $W(\mathbf{k}_\delta, \omega) = [\omega^2 - \omega_{k_\delta}^2 - \text{Re} \Sigma_s^{(2)}(\mathbf{k}_\delta, \omega)]^2 \sim 0$  at some critical wavevectors  $\pm \mathbf{k}_\delta$  in low energies, the IC peaks appear; then the weight of the IC peaks is dominated by the inverse of the imaginary part of the dressed spinon self-energy  $1/\text{Im} \Sigma_s^{(2)}(\mathbf{k}_\delta, \omega)$ . Thus the positions of the IC peaks are determined by both functions  $W(\mathbf{k}, \omega)$  and  $\text{Im} \Sigma_s^{(2)}(\mathbf{k}, \omega)$ , where the zero points of  $W(\mathbf{k}, \omega)$  (then the critical wavevectors  $\mathbf{k}_\delta$ ) are doping dependent. Near the half-filling, the zero point of  $W(\mathbf{k}, \omega)$  locates at the AF wavevector  $[1/2, 1/2]$ , so the commensurate AF peak appears there. With doping, the holes disturb the AF background. Within the partial CSS framework, as a result of the self-consistent motion of the dressed holons and spinons, the IC magnetic correlation is developed beyond a

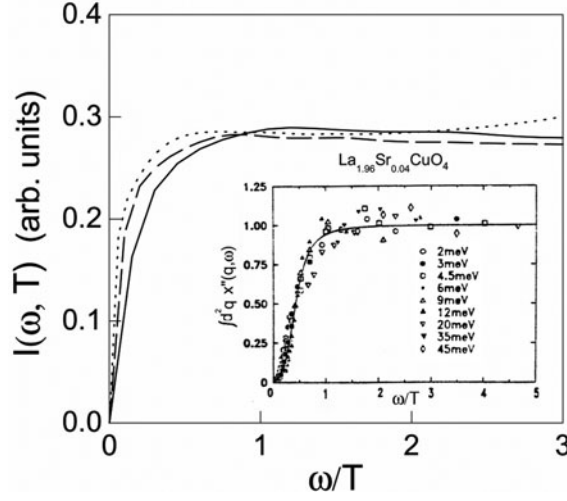


**Figure 7.** The integrated dynamical spin susceptibility at  $x = 0.12$  with  $t/J = 2.5$  and  $t'/t = 0.15$  in  $T = 0.2J$  (solid curve),  $T = 0.3J$  (dashed curve), and  $T = 0.5J$  (dotted curve). Inset: the experimental result for  $\text{La}_{2-x}\text{Sr}_x\text{CuO}_4$  taken from [9].

certain critical doping; this reflects the fact that the low energy spin excitations drift away from the AF wavevector, or the zero point of  $W(\mathbf{k}_\delta, \omega)$  is shifted from  $[1/2, 1/2]$  to  $\mathbf{k}_\delta$ . As is seen from equation (24), the physics is dominated by the dressed spinon self-energy renormalization due to the dressed holon pair bubble. In this sense, the mobile dressed holons are the key factor leading to the IC magnetic correlation, i.e., the mechanism of the IC type of structure in doped cuprates is most likely related to the dressed holon motion. This is why the position of the IC peaks can be determined in the present study within the  $t-t'-J$  model, while the dressed spinon energy dependence is ascribed purely to the self-energy effects which arise from the dressed holon–spinon interaction. Since the values of  $\text{Im } \Sigma_s^{(2)}(\mathbf{k}, \omega)$  increase with increasing energies, then all values of  $1/\text{Im } \Sigma_s^{(2)}(\mathbf{k}, \omega)$  are very small at high energies, which leads to the IC peaks disappearing at high energies.

## 6. Summary and discussions

In summary, we have developed a partial CSS fermion-spin theory to study the physical properties of the underdoped cuprates. In this approach, the physical electron is decoupled completely as the dressed holon and spinon, where the dressed holon keeps track of the charge degree of freedom together with the phase part of the spin degree of freedom, while the dressed spinon keeps track of the amplitude part of the spin degree of freedom. The local electron constraint for single occupancy is satisfied in analytical calculations. The dressed holon is a magnetic dressing, and it behaves like a spinful fermion, while the dressed spinon is neither boson nor fermion, but a hard-core boson. Moreover, both dressed holon and spinon are gauge invariant, and in this sense, they are real and can be interpreted as physical excitations. In the common decoupling scheme, we obtain the full dressed holon and spinon Green functions by using the equation of motion method.

Within this theoretical framework, we have studied the charge and spin dynamics of the underdoped cuprates based on the  $t-t'-J$  model. The conductivity spectrum contains a non-Drude low energy peak and a broad midinfrared band, while the temperature dependent

resistivity is characterized by a crossover from the moderate temperature metallic-like to the low temperature insulating-like behaviour in the heavily underdoped regime, and a temperature linear dependence with deviations at low temperatures in the underdoped regime. The commensurate neutron scattering peak at the half-filling is split into IC peaks with dopings, where the incommensurability is doping dependent, and increases with hole doping concentration at lower dopings, and saturates at higher dopings. These results are qualitatively similar to those seen in experiments. It is essential that these theoretical results were obtained without any adjustable parameters. These results also show that the charge dynamics is mainly governed by the scattering from the dressed holons due to the dressed spinon fluctuation, while the scattering from the dressed spinons due to the dressed holon fluctuation dominates the spin dynamics. In this case, the spin and charge dynamics in the normal state are almost independent, and the perturbations that interact primarily with the charge do not greatly affect the spin [21]; therefore the notion of partial CSS naturally accounts for the qualitative features of the normal state of the underdoped cuprates.

Based on this partial CSS fermion-spin theory, we have discussed the mechanism of HTSC in doped cuprates [41]. It is shown that dressed holons interact occurring directly through the kinetic energy by exchanging the dressed spinon excitations, leading to a net attractive force between the dressed holons; then the electron Cooper pairs originating from the dressed holon pairing state are due to the charge–spin recombination, and their condensation reveals the superconducting ground-state. The electron superconducting transition temperature is determined by the dressed holon pair transition temperature, and is proportional to the hole doping concentration in the underdoped regime. To our present understanding, the main reasons why the present theory is successful in studying the physical properties of doped cuprates are as follows.

- (1) The local electron constraint is exactly obeyed during analytical calculations in contrast with the slave-particle approach, where the local constraint is explicitly replaced by a global one [2, 29]. In this case, the representation space in the slave-particle approach is much larger than the representation space for the physical electron.
- (2) Since the extra  $U(1)$  gauge degree of freedom related with the local constraint has been incorporated into the dressed holon, this leads to the fact that the dressed holon and spinon are gauge invariant in the partial CSS fermion-spin theory. However, the bare holon and spinon in the slave-particle theory are strongly coupled by the  $U(1)$  gauge field fluctuation; they are not gauge invariant.
- (3) The representation of the dressed spinon in terms of the spin raising and lowering operators is essential in the present approach [29], because whenever a dressed holon hops it gives rise immediately to a change of the spin background as a result of careful treatment of the constraint given in section 2.

This is why the dressed holon–spinon interaction (kinetic part) dominates the essential physics of the underdoped cuprates [31, 38].

### Acknowledgments

The authors would like to thank Professors Z Q Huang, Z B Su, L Yu, Dr F Yuan, and Professor Z X Zhao for the helpful discussions. This work was supported by the National Natural Science Foundation of China under Grant Nos 10125415 and 10074007.



## References

- [1] See, e.g., Kastner M A *et al* 1998 *Rev. Mod. Phys.* **70** 897 and references therein
- [2] See, e.g., Bedell K S *et al* (ed) 1990 *Proc. Los Alamos Symp.* (Redwood city, CA: Addison-Wesley)
- [3] Anderson P W 1987 *Frontiers and Borderlines in Many Particle Physics* ed R A Broglia and J R Schrieffer (Amsterdam: North-Holland) p 1  
Anderson P W 1987 *Science* **235** 1196
- [4] See, e.g., Anderson P W 1997 *The Theory of Superconductivity in the High- $T_c$  Cuprates* (Princeton, NJ: Princeton University Press) and references therein
- [5] Rossat-Mignod J *et al* 1991 *Physica C* **185–189** 86
- [6] Birgeneau R J *et al* 1989 *Phys. Rev. B* **39** 2868
- [7] Yamada K *et al* 1998 *Phys. Rev. B* **57** 6165 and references therein
- [8] Dai P *et al* 2001 *Phys. Rev. B* **63** 054525 and references therein
- [9] Keimer B *et al* 1992 *Phys. Rev. B* **46** 14034
- [10] Sternlieb B J *et al* 1993 *Phys. Rev. B* **47** 5320  
Birgeneau R J *et al* 1992 *Z. Phys. B* **87** 15
- [11] Orenstein J *et al* 1990 *Phys. Rev. B* **42** 6342  
Tanner D B and Timusk T 1992 *Physical Properties of High Temperature Superconductors* vol 3, ed D M Ginsberg (Singapore: World Scientific) p 363 and references therein
- [12] Uchida S 1997 *Physica C* **282–287** 12 and references therein
- [13] Takagi H *et al* 1992 *Phys. Rev. Lett.* **69** 2975
- [14] Ando Y *et al* 2001 *Phys. Rev. Lett.* **87** 017001  
Ando Y *et al* Preprint cond-mat/0208096
- [15] See, e.g., Shen Z X and Dessau D S 1995 *Phys. Rep.* **253** 1  
Damascelli A, Shen Z X and Hussain Z 2003 *Rev. Mod. Phys.* **75** 473 and references therein
- [16] See, e.g., Dagotto E 1994 *Rev. Mod. Phys.* **66** 763 and references therein
- [17] Haldane F D M 1980 *Phys. Rev. Lett.* **45** 1358  
Haldane F D M 1981 *Phys. Lett. A* **81** 153  
Solyom J 1979 *Adv. Phys.* **28** 201
- [18] Yokoyama H and Ogata M 1991 *Phys. Rev. Lett.* **67** 3610  
Assaad F F and Würtz D 1991 *Phys. Rev. B* **44** 2681
- [19] Kim C *et al* 1996 *Phys. Rev. Lett.* **77** 4054
- [20] See, e.g., Maekawa S and Tohyama T 2001 *Rep. Prog. Phys.* **64** 383 and references therein
- [21] Anderson P W 1991 *Phys. Rev. Lett.* **67** 2092  
Anderson P W 2000 *Science* **288** 480  
Anderson P W 2001 Preprint cond-mat/0108522
- [22] Hill R W *et al* 2001 *Nature* **414** 711
- [23] Furukawa N *et al* 1998 *Phys. Rev. Lett.* **81** 3195  
Maekawa S and Tohyama T 1998 *J. Phys. Chem. Solids* **59** 1897
- [24] Martins G B *et al* 1999 *Phys. Rev. B* **60** R3716  
Martins G B *et al* 2000 *Phys. Rev. B* **63** 014414  
Martins G B *et al* 2000 *Phys. Rev. Lett.* **84** 5844
- [25] Laughlin R B 1997 *Phys. Rev. Lett.* **79** 1726  
Laughlin R B 1995 *J. Low. Temp Phys.* **99** 443
- [26] Zhang F C and Rice T M 1988 *Phys. Rev. B* **37** 3759
- [27] Rice T M 1997 *Physica C* **282–287** xix and references therein
- [28] Gros C, Joynt R and Rice T M 1987 *Phys. Rev. B* **36** 381
- [29] Feng S, Su Z B and Yu L 1994 *Phys. Rev. B* **49** 2368  
Feng S, Su Z B and Yu L 1993 *Mod. Phys. Lett. B* **7** 1013
- [30] Wiegmann P B 1988 *Phys. Rev. Lett.* **60** 821
- [31] Feng S and Yuan F 2001 *Symp. on the Frontiers of Physics at Millennium* ed Y L Wu and J P Hsu (Singapore: World Scientific) p 221  
Feng S, Yuan F, Yu W and Zhang P 1999 *Phys. Rev. B* **60** 7565
- [32] Plakida N M 2002 Preprint cond-mat/0210385
- [33] Zubarev D N 1960 *Sov. Phys.—Usp.* **3** 201
- [34] Keimer B *et al* 1992 *Phys. Rev. B* **46** 14034  
Matsuda M *et al* 2000 *Phys. Rev. B* **62** 9148
- [35] Feng S and Song Y 1997 *Phys. Rev. B* **55** 642

- [36] Kondo J and Yamaji K 1972 *Prog. Theor. Phys.* **47** 807
- [37] See, e.g., Tyablikov S V 1967 *Method in the Quantum Theory of Magnetism* (New York: Plenum)
- [38] Feng S and Huang Z 1998 *Phys. Rev. B* **57** 10328  
Yuan F, Feng S, Su Z-B and Yu L 2001 *Phys. Rev. B* **64** 224505
- [39] Zaanen J and Gunnarsson O 1989 *Phys. Rev. B* **40** 7391  
Poilblanc D and Rice T M 1989 *Phys. Rev. B* **39** 9749  
Schulz H J 1990 *Phys. Rev. Lett.* **64** 1445  
Bulut N, Hone D, Scalapino D J and Bickers N E 1990 *Phys. Rev. Lett.* **64** 2723  
Tanamoto T, Kohno H and Fukuyama H 1994 *J. Phys. Soc. Japan* **63** 2739  
Hasegawa Y and Fukuyama H 1987 *Japan. J. Appl. Phys.* **26** L322
- [40] Mook H A *et al* 1993 *Phys. Rev. Lett.* **70** 3490  
Fong H F *et al* 1999 *Nature* **398** 588  
He H *et al* 2002 *Science* **295** 1045
- [41] Feng S 2003 *Phys. Rev. B* **68** 184501